https://doi.org/10.5194/egusphere-2024-3800
Preprint. Discussion started: 9 January 2025

Improved Formulation of Fragmentation of Snow during Collision with Graupel/Hail based on Observations at Jungfraujoch: Cold Non-Dendritic Regime of Temperature

Freddy P. Paul[1], Martanda Gautam[1,2], Deepak Waman[1,3], Sachin Patade[1], Ushnanshu Dutta[1,4], Christoffer Pichler[1], Marcin Jackowicz-Korczynski[1], Vaughan Phillips[1,4]

[1]Department of Physical Geography and Ecosystem Science, Lund, Sweden
[2]Institute of Atmospheric Physics, Johannes Gutenberg University, Mainz, Germany
[3]Institute of Meteorology and Climate Research, Karlsruhe Institute of Technology, Karlsruhe, Germany
[4]Department of Atmospheric Sciences, National Taiwan University, Taipei, Taiwan

Correspondence to: Vaughan Phillips (vaughan.phillips@nateko.lu.se)

Abstract. Much of the initiation of ice particles in deep precipitating clouds has been attributed to Secondary Ice Production (SIP). Fragmentation during collisions among particles of ice precipitation is one of the known SIP processes. Some recent studies have used our theoretical formulation of this SIP process in the cloud microphysics scheme of numerical atmospheric models published in 2017. However, there has been a lack of observational data for better understanding of the SIP process. The focus of the present study is on fragmentation of naturally falling snowflakes during their collisions with graupel/hail particles, based on observations conducted at Jungfraujoch, a mountain pass in the Alps and located about 3.6 km above Mean Sea Level. The cloud-top was at about -25^{o} to -32^{o} C. The study used a portable chamber specially designed to observe the fragmentation of snow particles outdoors. Fixed ice spheres in the chamber were used to mimic graupel or hail. Based on the observational study, we optimised the theoretical formulation for prediction of the number of fragments arising from collisions between snow and graupel/hail. The observations reveal an average number of fragments per collision of about 5. The study improved the prediction of SIP by this type of fragmentation compared to our original theoretical formulation, for snow consisting of mostly aggregates of crystals from the 'non-dendritic habit regime' of temperatures colder than -17^{o} C.

1 Introduction

Clouds play a pivotal role in controlling the weather and climate of the Earth's atmosphere. Climatological studies show that clouds act to cool the Earth's atmosphere by about 20^{o} C (Liou 2002). However, clouds pose several challenges to atmospheric models, whether of fine or coarse resolution. For the realistic simulation of clouds, the weather and climate models require increasingly sophisticated representations of cloud microphysical properties, which are governed in nature by the concentrations, and hence mean sizes, of cloud-particles (Seifert and Beheng, 2006; Thompson and Eidhammer 2014; Tatsuya

https://doi.org/10.5194/egusphere-2024-3800
Preprint. Discussion started: 9 January 2025

Seiki and Satoh, 2022; Zhao *et al*., 2024; Huang *et al*., 2024; Schäfer *et al*., 2024). This understanding has led to a recognition of the importance of aerosol-sensitive cloud microphysics in the macrophysical evolution of cloud ensembles and their associated precipitation. Specifically, the ice particle concentration within the clouds can influence a cloud's life time, surface precipitation and its radiative and microphysical characteristics, affecting also the mean sizes and hence morphology of ice particles (Gettelman *et al*., 2012; Fan *et al*., 2017; Cesana and Storelvmo, 2017; Heymsfield *et al*., 2020).

Airborne observations of ice particle concentrations in precipitating clouds are found to exceed the ice nucleating particle (INP) concentrations by several orders of magnitude, even when the cloud top is too warm for homogeneous freezing (Hobbs and Rangno, 1985; Mossop, 1985; Cantrell and Heymsfield, 2005; DeMott *et al.*, 2016). Different processes have been identified for this discrepancy between ice number concentration and INPs (Hobbs and Rangno, 1985; Beard and Kenneth, 1992; Fridlind *et al*., 2007). These processes include pre-activated INPs (Fridlind *et al.*, 2007), thermophoretically enhanced contact-freezing (Hobbs and Rangno, 1985; Beard and Kenneth, 1992), and some physical processes capable of generating new ice crystals by 'secondary ice production (SIP)'. SIP creates new ice crystals in the presence of pre-existing ice particles without the action of INPs or homogeneous freezing (Field *et al*., 2017). Over the past several decades, several SIP mechanisms have been identified: (1) shattering during freezing of raindrops or drizzle, (2) the rime-splintering (Hallett–Mossop) process, (3) fragmentation due to ice–ice collision, (4) ice particle fragmentation due to thermal shock, (5) fragmentation of sublimating ice, and (6) activation of ice-nucleating particles in transient supersaturations around freezing drops. A recent idea involves evaporation of drops, which can cool them by many degrees Celsius, perhaps facilitating their freezing heterogeneously (Roy *et al*. 2024).

Fragmentation in ice–ice collisions is the main source of SIP over time-scales longer than a few 10s of minutes according to detailed simulations (e.g., domain of 100 × 100 km wide) of mesoscale convective systems, which have been shown to agree with aircraft and ground-based data (Phillips *et al*. 2017b; Huang et al. 2021; Waman *et al*. 2022), (see also Zhao and Liu, 2021). Such recent models are initialized with a representation of the environmental aerosol conditions, reproducing the coincident active INP concentration, and predict with adequate accuracy the average concentrations of ice particles in-cloud sampled by aircraft. The process of breakup in ice-ice collisions is vital for this accuracy and yet has not been treated in most other atmospheric models, partly due to scarcity of observational data historically. But also the inherent complexity of the breakup process is a factor. The variety of possible morphologies of ice precipitation creates complexity from many permutations of types of pairs of colliding particles. Each permutation of morphologies of colliding particle would be expected to yield different intensities of fragmentation. Snowflake aggregates are especially prone to fragmentation because they consist of crystal monomers with asperities that interlock, with a low bulk density and high fragility. This complexity is a challenge for empirical characterization of the breakup process.

https://doi.org/10.5194/egusphere-2024-3800
Preprint. Discussion started: 9 January 2025

Phillips *et al*. (2017a) provided a comprehensive numerical formulation for the SIP mechanism of fragmentation in ice-ice collisions for any permutation of microphysical species of colliding particles. This formulation was based on observations from a few laboratory/field studies and on theoretical considerations from the classical mechanics of collisions, involving concepts such as the energy budget of a collision and Newton's law of restitution. Phillips *et al*. (2017b) implemented the formulation in a cloud model with a mesoscale domain (e.g. 100 km wide) and showed that most of the ice crystals formed in the mixed-phase part of the convective storms were from this break-up in ice-ice collisions. Budgets showed that most (> 90%) of the secondary ice particles were from fragmentation in collisions of snow (e.g. aggregates) with graupel/hail, especially in deep convective cores. The formulation was also implemented in simulations of Arctic clouds with a global model (Sotiropoulou *et al*., 2021). The observational basis for the formulation was only preliminary as the observations were from Vardiman's (1978) data from the 1970s, on contrast with the modern technology used here.

In the quest for better understanding of this prolific SIP mechanism involving collisions of snow particles with hail/graupel, outdoor observations of naturally falling snow at the ground have been performed for the present study. A specially designed portable laboratory chamber, (Gautam 2022; Gautam *et al.* 2024) is used to study the fragmentation of naturally falling snow. Our modeling noted above has identified snow vs graupel/hail as the most prolific permutation of colliding microphysical species for fragmentation (Phillips *et al.* 2017b). Observations outdoors with the chamber provides a basis for a more accurate empirical formulation of snow fragmentation in atmospheric models. Deployment of the probe at a mountain-top laboratory reduced the likelihood of sublimational breakup, and weakening of snow by partial sublimation, during fall-out of snow through the ice-subsaturated environment below cloud. That problem was discussed by Phillips *et al*. (2017a).

The structure of the paper is as follows. The next section shows the methodology of the observations with emphasis on the chamber design and inference of fundamental parameters from the data. In the subsequent section, a brief description of the theoretical formula of SIP based on Phillips *et al*. (2017b) is summarised. Finally, results are shown from the improved formulation, optimized by re-fitting it to the new observations. Idealized simulations are shown to reveal some key dependencies of the new scheme. Conclusions of the study are discussed in the concluding section.

2 Methodology

The portable laboratory chamber has dimensions of 30 cm in width and 40 cm in height (Fig. 1). It is deployed outdoors to observe the fragmentation of snowflakes. The design of the chamber is described by Gautam (2022) and Gautam *et al*. (2024). It is a modern version of the experimental set up by Vardiman (1978). The chamber of Vardiman had metal surfaces acting as a colliding surface for naturally falling snowflakes. However, in the present study our chamber has used ice spheres fixed at the base of the chamber as the colliding surface, thereby more nearly replicating the morphology of hail/graupel particles. There are 126 ice spheres separated by 2 cm and arranged horizontally at the middle of the chamber.

https://doi.org/10.5194/egusphere-2024-3800
Preprint. Discussion started: 9 January 2025

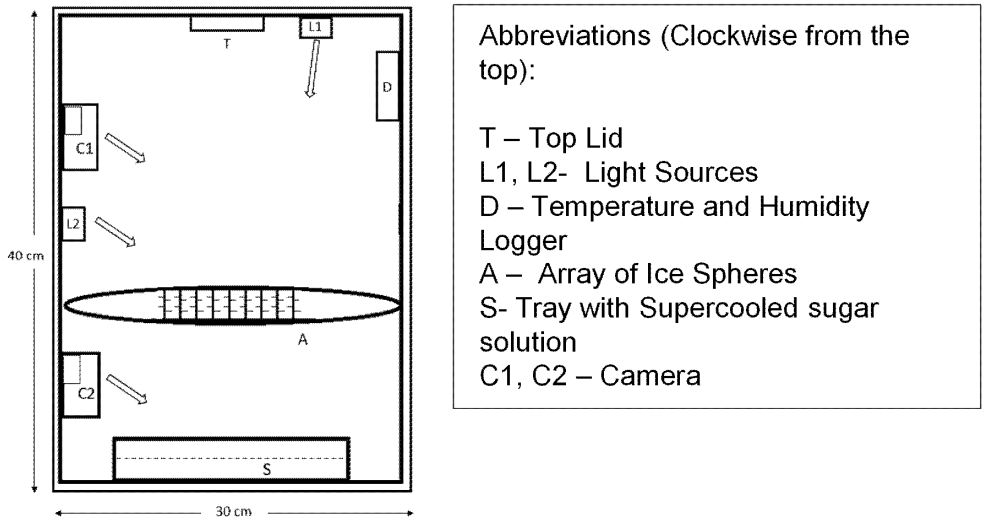

Figure 1: Design of the portable laboratory chamber for observing collisions between incident snowflakes and ice spheres that mimic graupel/hail particles. A vertical section through the chamber is shown. Reproduced from Gautam et al. (2024) with permission from the American Meteorological Society, USA.

2.1 Study area and prevalent meteorological conditions

The collection of data and sampling for the study were carried out at the top of the at Jungfraujoch mountain in the Alps (46.54° N and 7.86° E) at an elevation of 3.6 km above Mean Sea Level (MSL). This is a snow saddle area with an almost flat southern side. The northern side is vertical with a height difference of 3 km from the bottom of the valley. The snowfall event happened on 5-6 March 2024. The sampling of snow was performed on the open terrace of Jungfraujoch Sphinx Observatory on 5 March. Satellite observations from the European Organisation for the Exploitation of Meteorological Satellites (EUMETSAT) showed cloud-top temperatures between −25° and −32° C over the mountain on 5 March. The surface air temperature at the sampling site was about −4° C and the relative humidity was 27%. Locally on the terrace of the observatory where we sampled, there was little or no horizontal wind during the measurement. A deck of nimbostratus cloud was the source of the snow.

The snowflakes observed were mainly non-dendritic in structure. Figure 2 shows typical images of snowflakes at the study site during the time of observation.

https://doi.org/10.5194/egusphere-2024-3800
Preprint. Discussion started: 9 January 2025

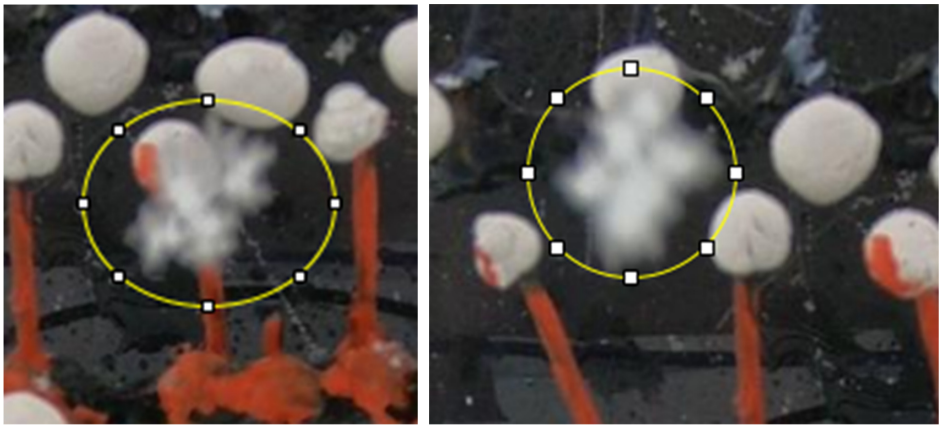

Figure 2: Images of typical non-dendritic snowflakes, inside the circle, observed at the study site, Jungfraujoch, during the time of measurement on 5 March 2024.

120

2.2 Working of the chamber

Figure 1 shows the design of the chamber in a vertical section. It has a small rectangular opening on its top with a lid to control the entry of falling snow into it outdoors. When the lid is opened, a few snow particles would fall into the chamber and 125 fragments would be emitted from collisions with the fixed ice spheres arranged inside it. To record the fragmentation of snow two high speed cameras (GoPro 6, 120/second frame rate) were installed inside the chamber. Videos of fragmentation of the snow were recorded. After the trip, visual inspection of the videos enabled numbers of fragments in each collision to be counted and the fall speeds and sizes of incident snowflakes to be measured. The chamber was kept outside for 20 to 30 minutes for thermal stabilization before sampling began.

130

The representativeness of ice spheres to mimic graupel/hail in its collisions with snow is not perfect since their surface is not rimed. However, fragmentation in any ice-ice collision is expected to be of the more fragile particle in the pair, and so collisions of snow with either fixed ice spheres or graupel/hail aloft must involve fragmentation of only the snow particle. So the morphology of the graupel/hail is not expected to be so influential for the fragmentation of the snow. The bulk density of 135 graupel/hail exceeds that of snow for all sizes, so the snow particle must generally always be more fragile than the graupel/hail in any collision; this bulk density generally tends to increase with graupel/hail size, even approaching that of pure ice for sizes bigger than about 1 or 2 cm, due to the density of accreted rime increasing with impact speed (Pruppacher and Klett 1997; Gautam *et al*. 2024, their Appendix C). The fact that the ice spheres are fixed and cannot rebound, in contrast with natural graupel/hail in-cloud aloft, is immaterial because the experimental data is analysed in terms of collision kinetic energy (CKE),

https://doi.org/10.5194/egusphere-2024-3800
Preprint. Discussion started: 9 January 2025

which is the fundamental determinant of the fragmentation according to classical mechanics (Phillips *et al*. 2017a), (see also Testik *et al.* 2011). Each fragment requires a certain amount of energy to create its surface energy, and there cannot be more fragments created than are allowed by the initial CKE, after allowing for other losses of energy.

More details regarding the working of the portable laboratory chamber are provided by Gautam (2022) and Gautam *et al.* (2024). The following subsections explain data sampling, data processing, empirical parameter estimation, and the calculations of CKE and rime fraction.

2.3 Snow sampling to estimate mass-size relation

To infer the mass of any snow particle undergoing fragmentation in the chamber, a practical method was to infer it from the size measured from the video footage in the chamber. This necessitated knowing the mass-size relation of the snow. However, generally, in view of the complexity of morphology of ice precipitation, the mass-size relations of snow crystals and aggregates can vary widely (e.g. Pruppacher and Klett 1997). Consequently, it was necessary to measure the mass-size relation of the falling snow at the sampling site during the snowfall event.

Following Gautam *et al.* (2024), to estimate this average relation between the mass and maximum dimension of the falling snow flakes, snow samples were collected inside two cylindrical plastic containers (7 cm height and 5 cm diameter) outside the chamber. These two plastic containers were cleaned and dried prior to the sampling of the snow. The dry weights of both containers were measured using a weighing balance. These bottles with open lids were exposed to snowfall for almost 1 minute under a video camera and sealed tight. The weights of both bottles were again calculated to infer the mass of the collected snow in each. The mass-size power relation was then estimated by numerical variational analysis using the total measured masses of the collected snow in both capsules and observed sizes of all the individual snowflakes as they fell into the capsules from the video.

2.4 Raw data processing

The collisions and fragmentation of the snowflakes are analysed carefully using ImageJ software. The distortion corrections are made and the images of each collision event are extracted. Sizes and numbers of fragments from each collision are calculated from the extracted images using this software. The fall speeds of incident snow particles before collisions are calculated by inspecting the videos with the software. Even with utmost care and corrections, some errors arise while measuring the fall speed and thereby CKE. Any errors associated with the measurements would introduce errors in the prediction of SIP after fitting it to the observations.

https://doi.org/10.5194/egusphere-2024-3800
Preprint. Discussion started: 9 January 2025

2.5 Empirical parameter estimation and CKE calculation

In order to calculate CKE, the empirical parameters present in the relation connecting snow flake size with its fall speed and mass are estimated from the data extracted from the video recordings. The mass-size relation is as shown below.

$$m = aD^b , \quad (1)$$

In Eq (1), m and D are the mass and maximum dimension of the colliding snowflake respectively, while a and b are empirical parameters. The mass-size relation yielded the mass of each incident snowflake inside the chamber before impact on an ice sphere, using the measured size from the video. This mass was then combined with the fall speed, inferred from the video inside the chamber, to yield the CKE.

2.6 Calculation of rime fraction

The 'rime fraction' is the fraction of mass of a snow particle acquired by riming of supercooled cloud-liquid. In the formulation of breakup in ice-ice collisions, prediction of the number of secondary ice particles (Eq (2) below) requires the rime fraction of the incident ('parent') snowflake as an input. To estimate the rime fraction of each snow particle, a detailed numerical simulation of clouds is performed. More specifically, a similar case of orographic clouds is simulated in a 3D mesoscale domain using the Aerosol-Cloud (AC) model (Phillips *et al*. 2017b; Waman *et al*. 2022). The AC model diagnoses the bulk value of rime fraction for the entire range of sizes of snow by tracking the component of snow mass that is rime.

The simulated case was observed during the experimental field campaign named ARM (Atmospheric Radiation Measurement) Cloud Aerosol Measurement (ACAPEX) on 7th February 2015, near California. Further details of the experimental set up and observational results are given by Leung (2016). The details of ACAPEX simulation by the AC model are described by Waman *et al*. (2022). From the ACAPEX simulation, cloudy columns having cloud-top (-25^o C to -32^o C) and surface air (-4^o C) temperatures similar to those of the site in the present study (Jungfraujoch) are selected and the bulk rime fraction is averaged conditionally over all selected columns. This bulk rime fraction then constrains the average relation of assumed form between the rime fraction and snow size (Sec. 3).

3 Description of Formulation for Breakup in Ice-ice Collisions

The essence of the formulation (Phillips *et al*., 2017a) for this type of SIP is:

$$N = \alpha\, A(\mathbf{M}) \left(1 - e^{-(CK_0/\alpha A(\mathbf{M}))^\gamma}\right) , \quad (2)$$

Here, N is the number of secondary ice particles per collision, α is the equivalent spherical surface area (m^2) of the smaller particle in the colliding pair, K_0 is the initial CKE (J), while $A(\mathbf{M})$ is a measure of the areal number density of breakable asperities of the more fragile of the colliding particles (m^{-2}) . Also $\gamma = 0.5 - 0.25\psi$ is a dimensionless exponent and C is

https://doi.org/10.5194/egusphere-2024-3800
Preprint. Discussion started: 9 January 2025

asperity fragility coefficient (J^{-1}). Here, **M** is the vector of morphological properties of the colliding particles (e.g. shape, bulk density, porosity) and ψ is the rime fraction of the snow particle. The areal density of asperities is given by

$$A(\mathbf{M}) = \beta(1 + 100 \times \psi^2)(1 + \sigma/D^{1.5}) \quad (3)$$

Here, σ and β are empirical constants, and D (m) is the maximum dimension of the more fragile of the two colliding ice particles. D is thresholded, as the input for Eq (3), to be in the range from 5×10^{-4} to 5×10^{-3} m. Also, $\sigma = 1.33 \times 10^{-4}$ $m^{1.5}$. Finally, Phillips *et al*. (2017a) proposed an upper limit for N of 100 in view of the general lack of observations of fragmentation greater than this. Symbols are listed in Table A1 (Appendix A).

Parameter values for various permutations of microphysical species in the collision pair were proposed. These were treated as collisions of (a) graupel with graupel/hail, (b) hail with hail, (c) dendritic snow/crystals with any other type of ice precipitation, and (d) similarly for non-dendritic snow/crystals. The present study treats only collision type (d). As noted below (Sec. 7), the term 'dendritic' or 'non-dendritic' snow is to be interpreted broadly in terms of the likely temperature regime of growth of the component crystals and does not imply the snow particles necessarily are regular or pristine.

Regarding implementation of the formulation, it is best done by a system of bins to discretise the size distribution of the colliding species. The rime fraction ideally should be predicted somehow. If predicted in a bulk sense for snow particles of all sizes, then the value of rime fraction at any size can be diagnosed by assuming a linear form of its dependence on size (Gautam *et al*. 2024). Otherwise, a default value of rime fraction may be applied (e.g., 0.2).

4 Results for Observations of Snow Fragmentation

The snowfall on 5 March 2024 at Jungfraujoch lasted from early morning until the afternoon of the next day (Sec. 2.1). The snow consisted of mostly non-dendritic aggregates having maximum dimensions ranging from 0.1 to 1.3 cm. The surface air temperature was observed to be about -4^{o} C to -5^{o} C on both days while sampling at the observing station. The observed number of secondary ice fragments during each collision event was recorded by video, with a dataset of about 10^2 collisions in total.

The collision events were categorized into several bins based on the size of the parent snow particle. The average number of secondary ice particles per collision for each bin, N, is calculated and plotted as a function of the size of the parent snow particle, D_{Parent}, as shown in Fig. 3. There is a gradual increase in the number of secondary ice particles per collision with the size of the parent snow particle up to about 6 mm and then it decreases slowly at larger sizes. For the observed range of snow sizes from 0.15 to 1.3 cm, the average number of secondary ice particles produced per collision was observed to be about 5.

https://doi.org/10.5194/egusphere-2024-3800
Preprint. Discussion started: 9 January 2025

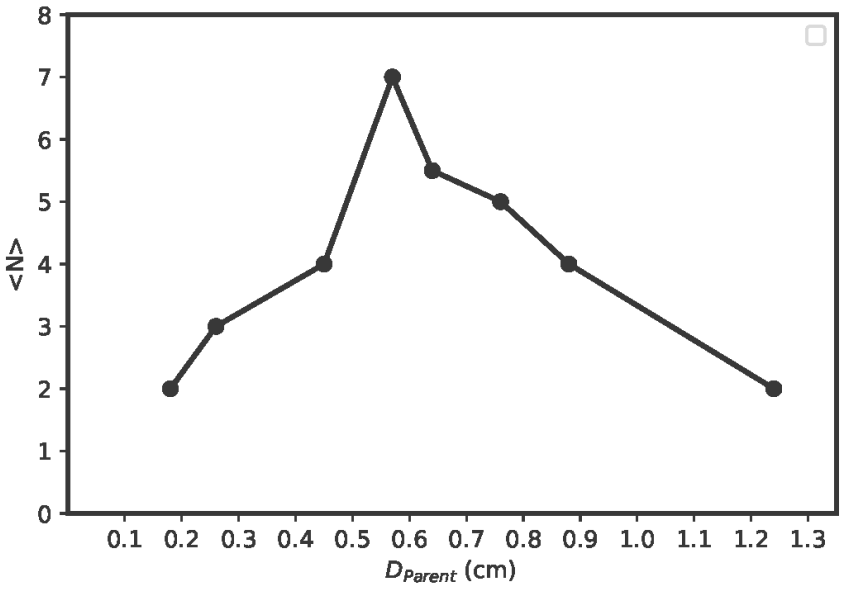

Figure 3: Distribution of number of secondary ice particles per collision, N, with the size of the parent snowflake, D_{Parent}, as observed inside the portable laboratory chamber on 5 March 2024 at Jungfraujoch.

235 Figure 4 shows the average size distribution of number of secondary ice particles per collision with their size, D_{frag}, after binning all fragments by size. Secondary ice fragments are most numerous at sizes of about 0.5 mm, which is about 20% of the mean value (2.5 mm) of size of the incident parent snow particles. The peak observed is well above the threshold value of detection (0.3 mm), which is consistent with almost all secondary ice fragments from each collision being visible and detected.

https://doi.org/10.5194/egusphere-2024-3800
Preprint. Discussion started: 9 January 2025

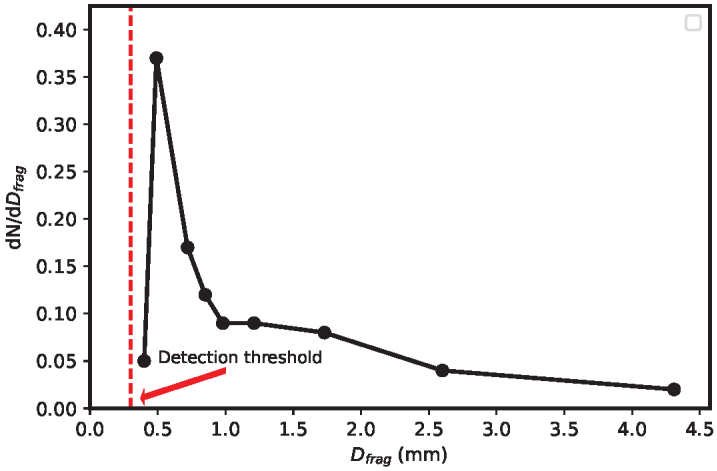

Figure 4: Fragment size distribution, dN/dD_{frag}, of secondary ice particles per collision during the collisional fragmentation of snow, as a function of their maximum dimension, D_{frag}, as observed inside the portable chamber on 5 March 2024 at Jungfraujoch. N is the total number of fragments per collision. The threshold value of detection of snow fragments is shown by the red dotted line.

This form of the size distribution of fragments is expected in view of statistical partitioning of surface energy as a conserved quantity among the fragments, akin to partitioning of kinetic energy among molecules of an ideal gas or of mass among cloud droplets.

Finally, the observations of fragmentation of snow are displayed in Fig. 5 (green points). There is a monotonic trend of N increasing with CKE, which in turn increases with parent snow size. Fall speeds were estimated with a 13% error (from the frame rate) while mass of any snow particle (inferred from the mass-size relation) has a 20% error (from the error in measuring size of 13% for the mass-size relation), implying a 46% error for CKE.

https://doi.org/10.5194/egusphere-2024-3800
Preprint. Discussion started: 9 January 2025

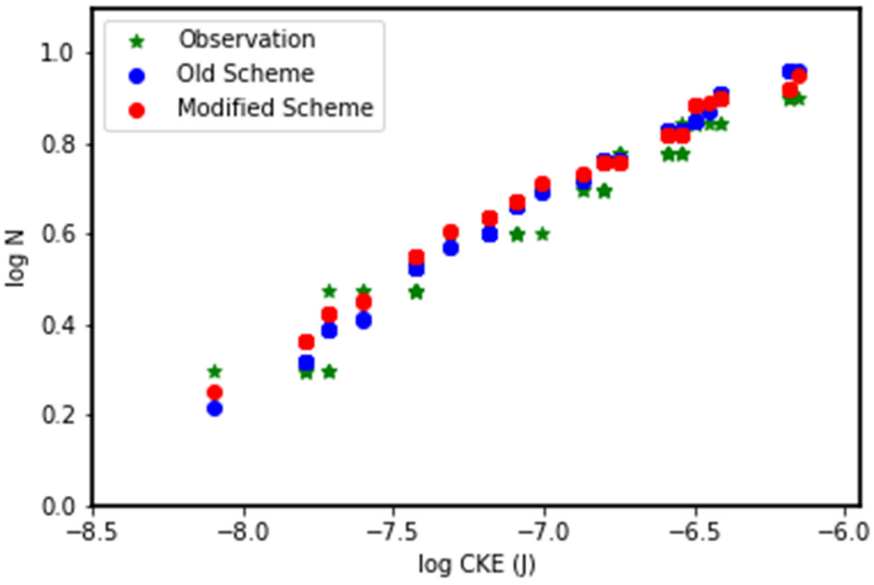

Figure 5: Comparison of variations of number of secondary ice particles per collision (N) as a function of collision kinetic energy (CKE) from old (Phillips *et al.*, 2017b) and new refitted (Table 1) schemes. The new scheme is from observations of collisional fragmentation made inside the portable chamber on 5 March 2024 at Jungfraujoch.

5 Results from Re-fitting the Formulation

The observations of snow fragmentation in the portable chamber (Sec. 4) have been used to modify the formulation (Sec. 3) of ice-ice collision breakup whenever it is applied to the type of snow sampled here. As the structure of the snowflakes is inferred to be mostly non-dendritic from the observed cloud-top temperature (-25^{o} to -32^{o} C), only the non-dendritic part of the formulation is re-fitted at temperatures colder than -17^{o} C. The fitting is done by simulating the breakup in each collision event with the formulation, using the observed values of size of the snow flakes, their kinetic energies, the inferred temperature for predominant crystal growth (cold non-dendritic region) within the clouds and the rime fraction as the input parameters. The value of rime fraction, estimated for the snow sampled at Jungfraujoch (Sec. 2.6), is 0.20.

The estimated values of the empirical parameters a and b (Sec. 2.5) are provided in Table 1 for the mass-size relation in Eq (1). They are used to estimate the mass of each falling snowflake in the chamber from its measured size, to constrain the CKE. The optimization of coefficients in the formulation of collision breakup is carried out by selecting many trial values for C and β in Eqs (2) and (3), spanning several orders of magnitude. The permutation of both values with the least root mean square error

https://doi.org/10.5194/egusphere-2024-3800
Preprint. Discussion started: 9 January 2025

for the fragment number for the entire set of sampled collisions (Sec. 4) is selected as the optimum value. The new optimised values for C and β from this re-fitting procedure are provided in Table 1.

Table 1: Estimated values of the empirical parameters in the mass-size relation (5-6 March 2024, Jungfraujoch), (Eq (1)) and the optimised refitted values for two parameters of the collision break-up formulation for the prediction of secondary ice particles from snow collisions with graupel/hail (Eqs (2) and (3)). The mode of formulation involves snow from crystals grown in the non-dendritic habit regime at temperatures colder than -17^{o} C.

Parameter	a	b	C	β
Estimated value	2.8×10^{-3} kg m^{-b}	1.5	2.9×10^{6} ($\pm$46%) J^{-1}	5.2×10^{5} ($\pm$26 %) m^{-2}

The new estimated values of C and β from Table 1 are used in the prediction of N in the formulation (Eqs (2) and (3), Sec. 3) for snow from non-dendritic crystals grown at temperatures colder than -17^{o} C. The corresponding unmodified values of other parameters are noted above (Sec. 3). The present study suggests a default value for ψ of 0.2, if it cannot be predicted in the atmospheric model. Symbols are listed and defined in Table A1 (Appendix A).

Figure 5 (red points) also shows the predicted values of number of secondary ice particles during collision fragmentation, for each observed collision event inside the portable chamber. Regarding the accuracy of the formulation for collision fragmentation for the non-dendritic case, the error in the prediction of N is around $\pm$ 50%, in view of errors in determining C and β (Table 1). The main sources of these errors in C and β were uncertainty in calculation of CKE from the raw observations (46%) and in measurement of the dimension of the colliding snow particles (13%).

The predicted numbers of secondary ice particles from Phillips *et al.* (2017b), hereafter referred to as the old scheme, is also shown in Fig. 5 (blue points) along with observations. There is a monotonic increase in the number of secondary ice particles for both old and newly fitted schemes as with the observations. Naturally, by design, the modified scheme shows good agreement with the observations used to construct it, over all the range of CKE values. For a given value of CKE, the prediction of number of secondary ice prediction differs from the observation with a root mean square error of $\pm$ 5 for the old scheme whereas it is $\pm$ 3 for the modified scheme. Thus, by design, the newly fitted formulation performs better in prediction of secondary ice particles during fragmentation than the old scheme.

Note that comparison of the prediction with observations in Fig. 5 is not a validation of the new scheme since they were used in its construction. Rather the comparison merely illustrates the goodness of the fitting procedure.

https://doi.org/10.5194/egusphere-2024-3800
Preprint. Discussion started: 9 January 2025

6 Results from Idealised Simulations of SIP

Three sets of idealised simulations of breakup in single snow-graupel collisions were done to elucidate the behavior of the formulation. The goal is to understand how the prediction of this type of SIP responds to variations in CKE (K_0), size of the parent snowflake (D_{Parent}) and rime fraction (ψ) for the modified scheme (Table 1, Sec. 5). This is done by varying each of these input quantities in isolation while keeping the other quantities fixed at their default values. These default values for the snow particle are: $D_{Parent} = 5$ mm (maximum dimension), $\psi = 0.2$, axial ratio of 0.3, and $K_0 = 10^{-7}$ J. Default values of the graupel particle are: 5 mm diameter and an axial ratio of 1 (spherical shape). Additionally, the same idealized sensitivity tests were performed for the old scheme (Phillips *et al*. 2017b). The default values yield $N = 12$.

Figure 6 shows the effect from varying CKE in isolation to examine the role of impact speed alone. This reveals a power-law dependence of N on K_0, with a monotonic increase of fragment number with CKE. For every order of magnitude increase in CKE, there is almost half an order of magnitude increase in N. This sensitivity is comparable to that seen in the observations (Fig. 5), which include effects from co-variation of area of impact (depending on snow size), rime fraction and CKE together. The implication is that most of the variation in fragmentation seen in our observations (Fig. 5) is explicable in terms of CKE increasing with larger particles due to their greater mass and impact speed. The modified and old schemes perform similarly with N being predicted to be only 20% higher with the new scheme.

https://doi.org/10.5194/egusphere-2024-3800
Preprint. Discussion started: 9 January 2025

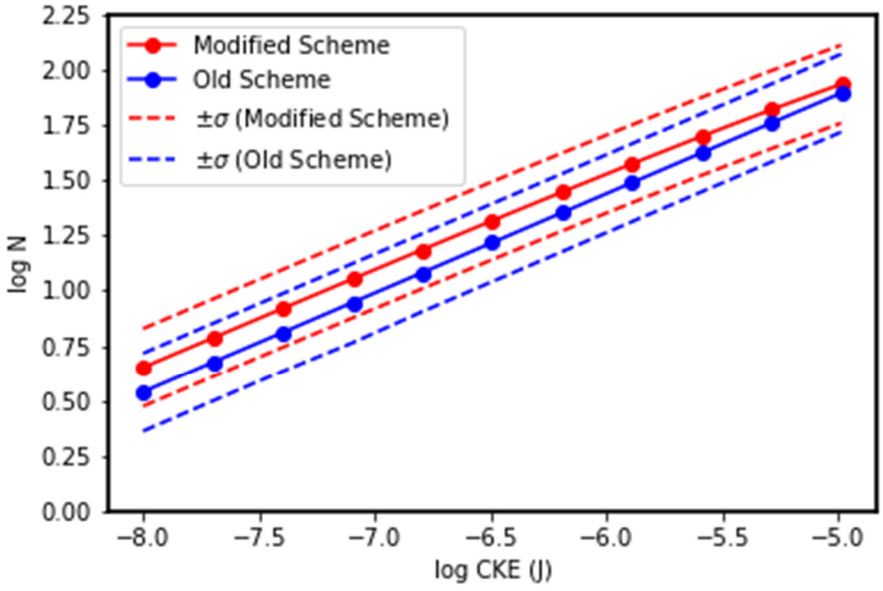

Figure 6: Response to varying collision kinetic energy (CKE) of number of secondary ice particles per collision (*N*) from new refitted (Table 1) scheme (red line), in the idealized sensitivity test. Also, shown is the old (Phillips *et al*., 2017b) scheme (blue line). Size of snow and rime fraction are held constant at default values. The broken lines represent one sigma standard deviation for modified and old schemes.

Figure 7 shows the variation of the number of secondary ice particles per collision with the size of colliding parent snow, D_{Parent}, for both schemes. This isolates the effect from area of impact controlling the number of asperities available for breaking. To that end, the CKE is artificially held constant. Of course, in nature the fallspeed would vary with size, altering the CKE. For diameters smaller than the default value, from 1 to 5 mm, there is a gradual increase in the predicted number of particles with increasing size. At the same time, above 5 mm there is a sudden increase in the number and it remained constant irrespective of the changes in the size of colliding parent snow. This is because the snow particle size controls α only when it is smaller than the graupel particle in the colliding pair (Sec. 3), which is 5 mm here. Over the entire range of sizes, there is only an increase by about half an order of magnitude. Again, the new prediction is about 20% higher than for the old scheme.

https://doi.org/10.5194/egusphere-2024-3800
Preprint. Discussion started: 9 January 2025

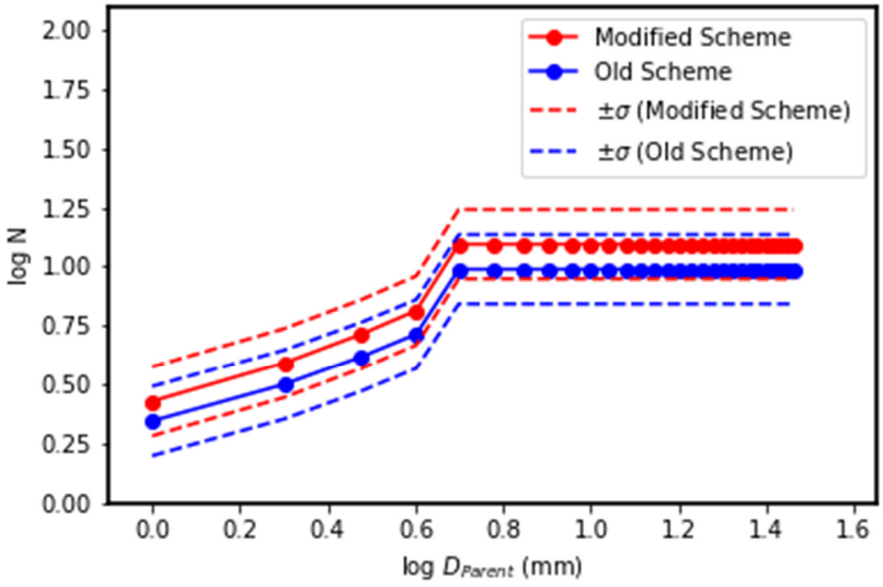

Figure 7: Effect from variation of colliding snow size (D_{Parent}) on predicted fragment numbers for the modified and old schemes for snow-graupel collisions, plotted as in Fig. 6.

Figure 8 shows the influence from rime fraction on the predicted SIP from both the modified and old schemes. From these idealised simulations, it can be inferred that there is a monotonic increase in the number of particles with the rime fraction by over an order of magnitude over the entire range of rime fraction (0.01 to 0.5). From $\psi = 0.01$ (with $N = 4$) to $\psi = 0.1$ (where $N = 6$), the prediction of N increases by 50%. From $\psi = 0.1$ to $\psi = 0.2$ (with $N = 12$) and then to $\psi = 0.5$ (yielding $N = 60$), it increases by factors of about 2 and 3. Thus, rime fraction is a sensitive input quantity in both new and old schemes. This sensitive dependency on rime fraction in the scheme (Eq (2), Sec. 3) was based on observations of lightly, moderately and heavily rimed snow particles by Vardiman (1978). Such studies (e.g. Gautam *et al*. 2024; Sec. 4), including the present one, have not attempted to measure rime fraction. Curiously, the new scheme has slightly less sensitivity to rime fraction than the old scheme, predicting twice the fragmentation at the lowest rime fraction of 0.01.

https://doi.org/10.5194/egusphere-2024-3800
Preprint. Discussion started: 9 January 2025

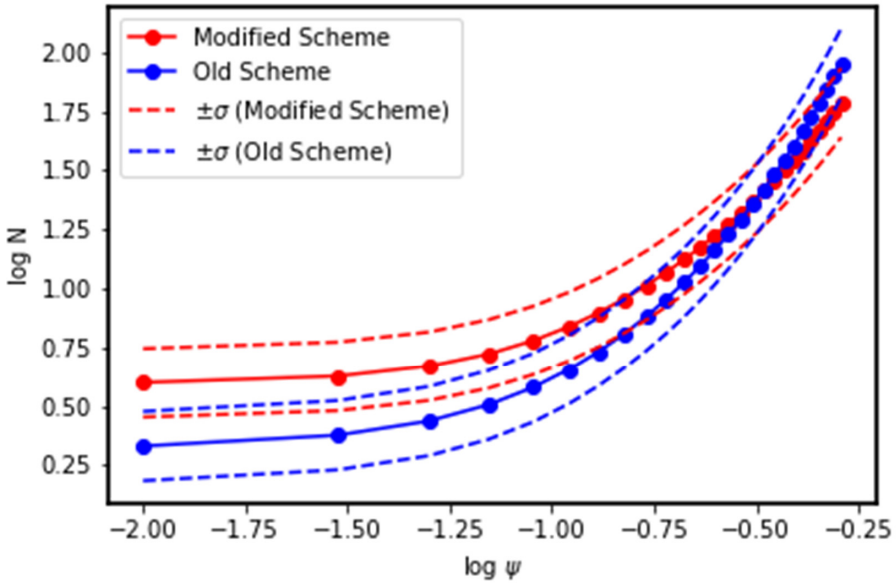

Figure 8: Response to varying the rime fraction (ψ) from idealised simulations of fragment numbers in snow-graupel collisions from modified and old schemes, plotted as in Fig. 6.

7 Conclusions

The SIP mechanism of fragmentation of snow in collision with graupel/hail has been empirically characterized by outdoor observations carried out at Jungfraujoch using a portable chamber. The concept of this chamber was inspired by the pioneering observations by Vardiman (1978). Our chamber uses modern technology and an array of ice spheres for representativeness, instead of the non-ice materials used by Vardiman. Snow particles fall into the chamber and individual collision events are filmed. The layer-cloud at Jungfraujoch producing the sampled snow had a top of between about -25^{o} to -30^{o} C, which suggests the snow aggregates will have been likely formed at levels above the dendritic region (-12^{o} to -17^{o} C). At such levels colder than -17^{o} C, the dominant habit of crystals would be expected to be the planar polycrystal (Bailey and Hallett 2009), the asperities of which would likely promote the sticking efficiency for ice-ice collisions and aggregation.

Thus, the observations of fragmentation correspond to that of 'non-dendritic snow' using the terminology of Phillips *et al.* (2017a) on the cold side of the dendritic region. Note that here the terms 'dendritic' and 'non-dendritic' snow do not imply

https://doi.org/10.5194/egusphere-2024-3800
Preprint. Discussion started: 9 January 2025

that the snow particles observed were somehow pristine, regular or consisting of pristine crystals. In fact, there were mostly aggregates of irregular structure and partly rimed, as is typical generally. Rather, this terminology is used only for a broad classification of all snow sampled and distinguishes between the temperature regions of growth of the snow particles and the likely habits of crystals accreted when forming them.

The mean number of fragments per collision involving the snow was observed to be 6. The peak of the fragment size distribution is seen to be about 20% of the mean parent size of 2.5 mm and is much higher than the detection threshold, indicating the realism of our measurements. In addition to this, the observations from Jungfraujoch have been used to update the formulation of snow fragmentation in collision with snow/graupel.

These observations were found to conform with the general form of dependencies represented by original formulation by Phillips *et al*. (2017b). However, the newly refitted formulation for non-dendritic crystals performs better than the original formulation. By design, the prediction of number of secondary ice particles by the new scheme is in good agreement with the observation with root mean square error for N of $\pm$ 2.8, indicating that the observations used to refit the scheme conform to its dependencies. However, the root mean square error for the original formulation was about $\pm$ 5.3 with respect to the observation. The average number of fragments per collision is about 5 for the new scheme but 3 for the old scheme.

Three sets of idealised simulations are also carried out to understand the variation of secondary ice particles with the CKE, size of parent snow and the rime fraction. The idealised simulation showed a consistent increase in the number of secondary particles per collision with the CKE, with almost half an order of magnitude increase in N for each order of magnitude in CKE. This resembles the sensitivity seen in the observations, consistent with CKE largely controlling the fragmentation in our dataset. Conversely, when CKE is artificially held constant, the number of secondary ice particles per collision showed an increase with the size of the parent snow while smaller than the colliding graupel particle. A much stronger sensitivity of N with respect to rime fraction is predicted, with an increase by an order of magnitude as rime fraction is varied between possible extremes.

To conclude, an improved formulation for the prediction of secondary ice from snow collisions with graupel/hail is proposed here for the cold (temperatures lower than -17° C) non-dendritic habit regime based on our outdoor observations at Jungfraujoch. The modified version of the formulation for the secondary ice prediction may be implemented in the cloud microphysics scheme of numerical atmospheric models. Regarding the accuracy of the formulation, the error in the prediction of N is about $\pm$ 50%. Future work should focus on measuring somehow the dependency on rime fraction, perhaps with modifications to the portable laboratory.

https://doi.org/10.5194/egusphere-2024-3800
Preprint. Discussion started: 9 January 2025

APPENDIX A

Table A1: List of symbols.

Symbol	Description	Unit
a	Empirical constant in mass-size relation for snow	kg m^{-b}
A	Measure of number density of breakable asperities in region of contact	m^{-2}
b	Empirical constant in mass-size relation for snow	-
C	Asperity fragility coefficient in formulation for breakup	J^{-1}
D	Maximum dimension of colliding snow particle in Eq (2) (thresholded to be between 0.5 and 5 mm)	m
D_{frag}	Maximum dimension of any fragment of ice	m
D_{parent}	The same as D, except in observations and without thresholding	m
K_0	Initial value of CKE before collision	J
m	mass of snowflake	kg
M	Vector denoting morphology of colliding particles and collision type	Multi-dimensional
N	Number of secondary ice particles per collision from breakup formulation	-
α	Surface area (equivalent spherical) of smaller particles	m^2
β	An empirical constant in expression for A related to areal density of asperities	m^{-2}
γ	Exponent for dimensionless energy in formulation for breakup	-

https://doi.org/10.5194/egusphere-2024-3800
Preprint. Discussion started: 9 January 2025

ψ	Fraction by mass of a snow particle or crystal that is rime	-
σ	An empirical constant in expression for A	$m^{1.5}$

Code and data availability: Unrestricted access to all data and software underlying our reported findings will be provided when the paper is published, using the project website at Lund University. Details on this access will be available from the lead author (FPP) on request.

Author contributions: FPP collected the observations, did the data analysis and wrote much of the paper. MG designed and developed the instrument. DM and SP contributed to the ACAPEX simulation used in the study. CP contributed to the data analysis of video footages. UD and MJK provided technical support for the data collection. VTJP designed and directed the study. All authors contributed to the scientific discussion and editing of the paper.

Competing interests: The authors declare that they have no competing financial interests nor any personal relationships that could have influenced the reported work in this paper.

Acknowledgements: We are grateful to Claudine Frieden for providing all facilities to conduct observation at Jungfraujoch observatory. We are also thankful to Thomas Furter and Sonja Stöckli for all the technical support while there. This work was chiefly supported by an award (2021-05547) to VTJP from the Swedish Research Council (VR), which concerns a study of the linkage between ice initiation and lightning using AI. UD was supported by an award (FR-2021/0005) to VTJP from the Swedish Research Council for Sustainable Development (FORMAS), while CP and SP were supported by an award to VTJP from Vinnova (2020-03406). DW was supported by another award to VTJP (FR-2018/0010) from FORMAS, regarding the modelling of ice initiation in clouds and climate.

References

Bailey, M. P., and Hallett, J.: A comprehensive habit diagram for atmospheric ice crystals: Confirmation from the Laboratory, AIRS II, and other field studies. *J. Atmos. Sci.*, **66**(9), 2888–2899, 2009.

Beard and Kenneth, V.: Ice initiation in warm-base convective clouds: An assessment of microphysical mechanisms, *Atmos. Res.*, **28,** 125–152, 1992.

https://doi.org/10.5194/egusphere-2024-3800
Preprint. Discussion started: 9 January 2025

Cantrell, W. and Heymsfield, A.: Production of ice in tropospheric clouds: A review, *Bull. Am. Meteorol. Soc.*, **86,** 795–808, 2005.

Cesana, G. and Storelvmo, T.: Improving climate projections by understanding how cloud phase affects radiation, *J. Geophys. Res.: Atmos*., **122,** 4594–4599, 2017.

DeMott, P. J., Hill, T. C., McCluskey, C. S., Prather, K. A., Collins, D. B., Sullivan, R. C., Ruppel, M. J., Mason, R. H., Irish, V. E., Lee, T., *et al*.: Sea spray aerosol as a unique source of ice nucleating particles, *Proc. Nat. Acad. of Sci.,* **113,** 5797–5803, 2016.

Fan, J., Leung, L. R., Rosenfeld, D., and DeMott, P. J.: Effects of cloud condensation nuclei and ice nucleating particles on precipitation processes and supercooled liquid in mixed-phase orographic clouds, *Atmos. Chem Phys.,* **17,** 1017–1035, 2017.

Field, P. R., Lawson, R. P., Brown, P. R., Lloyd, G., Westbrook, C., Moisseev, D., Miltenberger, A., Nenes, A., Blyth, A., Choularton, T., *et al*.: Secondary ice production: Current state of the science and recommendations for the future, *Meteorological Monographs,* **58,** 7–1, 2017.

Fridlind, A. M., Ackerman, A., McFarquhar, G., Zhang, G., Poellot, M., DeMott, P., Prenni, A., and Heymsfield, A.: Ice properties of singlelayer stratocumulus during the Mixed-Phase Arctic Cloud Experiment: 2. Model results, *J. Geophys. Res.: Atmos.*, **112,** 2007.

Gautam, M.: Fragmentation in graupel snow collisions, Master of Science dissertation, Dept of Physical Geography and Ecosystem Science, Lund University, Lund, Sweden, 2022.

Gautam, M., D. Waman, S. Patade, A. Deshmukh, V. T. J. Phillips, M. Jackowicz-Korczynski, P. Smith, and A. Bansemer: Fragmentation in graupel-snow collisions: new formulation from field observations. *J. Atmos. Sci.*, in press, 2024.

Gettelman, A., Liu, X., Barahona, D., Lohmann, U., and Chen, C.: Climate impacts of ice nucleation, *J. Geophys. Res.: Atmos.,* **117,** 2012.

Heymsfield, A. J., Schmitt, C., Bansemer, A., Gettelman, A., Field, P. R., Liu, C., *et al.*: Contributions of the liquid and ice phases to global surface precipitation: Observations and global climate modeling, J. Atmos. Sci., 77, 2629–2648, 2020.

Hobbs, P. V. and Rangno, A. L.: Ice particle concentrations in clouds, *J. Atmos. Sci.,* **42,** 2523–2549, 1985.

Huang, Y., Wu, W., McFarquhar, G. M., Wang, X., Morrison, H., Ryzhkov, A., Hu, Y., Wolde, M., Nguyen, C., Schwarzenboeck, A., Milbrandt, J., Korolev, A. V., and Heckman, I.: Microphysical processes producing high ice water contents (HIWCs) in tropical convective clouds during the HAIC-HIWC field campaign: evaluation of simulations using bulk microphysical schemes, *Atmos. Chem. Phys.*, **21,** 6919–6944, 2021.

Huang, S., Yang, J., Chen, Q., Li, J., Zhang, Q., and Guo, F.: Impact of secondary ice production on thunderstorm electrification under different aerosol conditions, *EGUsphere*, 2024, 1–32, https://doi.org/10.5194/egusphere-2024-2013, 2024.

Leung, L. R.: ARM Cloud-Aerosol-Precipitation Experiment (ACAPEX) Field Campaign Report, Tech. rep., DOE Office of Science Atmospheric Radiation Measurement (ARM) Program, 2016.

Liou, K. N.: *An introduction to atmospheric radiation*. Academic Press, 2002.

https://doi.org/10.5194/egusphere-2024-3800
Preprint. Discussion started: 9 January 2025

Mossop, S.: Secondary ice particle production during rime growth: The effect of drop size distribution and rimer velocity, *Q. J. R. Meteorol. Soc.,* **111,** 1113–1124, 1985.

Phillips, V. T., DeMott, P. J., and Andronache, C.: An empirical parameterization of heterogeneous ice nucleation for multiple chemical species of aerosol, J. Atmos. Sci., 65, 2757–2783, 2008.

Phillips, V. T., Yano, J.-I., and Khain, A.: Ice multiplication by breakup in ice–ice collisions. Part I: Theoretical formulation, *J. Atmos. Sci.*, **74,** 1705–1719, 2017a.

Phillips, V. T., Yano, J.-I., Formenton, M., Ilotoviz, E., Kanawade, 260 V., Kudzotsa, I., Sun, J., Bansemer, A., Detwiler, A. G., Khain, A., *et al*.: Ice multiplication by breakup in ice–ice collisions. Part II: Numerical simulations, *J. Atmos. Sci.*, **74,** 2789–2811, 2017b.

Pruppacher, H. R. and Klett, J. D.: *Microphysics of clouds and precipitation.* Kluwer Academic Publishers, Dordrecht, 1997.

Roy, P., Rauber, R. M., and L. Di Girolamo: Evolution of cloud droplet temperature and lifetime in spatiotemporally varying subsaturated environments with implications for ice nucleation at cloud edges. *Atmos. Chem Phys.,* **24,** 11653–11678, 2024

Schäfer, B., David, R. O., Georgakaki, P., Pasquier, J. T., Sotiropoulou, G., and Storelvmo, T.: Simulations of primary and secondary ice production during an Arctic mixed-phase cloud case from the Ny-Ålesund Aerosol Cloud Experiment (NASCENT) campaign, *Atmos. Chem Phys.*, **24,** 7179–7202, 2024.

Seifert, A. and Beheng, K. D.: A two-moment cloud microphysics parameterization for mixed-phase clouds. Part 1: Model description, *Meteorol. Atmos. Phys.,* **92,** 45–66, 2006.

Sotiropoulou, G., Ickes, L., Nenes, A., and Ekman, A.M.: Ice multiplication from ice–ice collisions in the high Arctic: sensitivity to ice habit, rimed fraction, ice type and uncertainties in the numerical description of the process, *Atmos. Chem Phys.*, **21,** 9741–9760, 2021.

Tatsuya Seiki, W. R. and Satoh, M.: Cloud Microphysics in Global Cloud Resolving Models, *Atmosphere-Ocean*, **60,** 477–505, 2022.

Testik, F. Y., Barros, A. P., and L. F. Biven: Toward a physical characterisation of raindrop collision outcome regimes, *J. Atmos. Sci*., **68,** 1097-1113, 2011.

Thompson, G. and Eidhammer, T.: A study of aerosol impacts on clouds and precipitation development in a large winter cyclone, *J. Atmos. Sci.*, **71,** 3636–3658, 2014.

Vardiman, L.: The generation of secondary ice particles in clouds by crystal–crystal collision, *J. Atmos. Sci.*, **35,** 2168–2180, 1978.

Waman, D., Patade, S., Jadav, A., Deshmukh, A., Gupta, A. K., Phillips, V. T., Bansemer, A., and DeMott, P. J.: Dependencies of four mechanisms of secondary ice production on cloud-top temperature in a continental convective storm, *J. Atmos. Sci.*, **79,** 3375–3404, 2022.

Zhao, J., Ma, X., Quaas, J., and Jia, H.: Exploring aerosol–cloud interactions in liquid-phase clouds over eastern China and its adjacent ocean using the WRF-Chem–SBM model, *Atmos. Chem Phys.,* **24,** 9101–9118, 2024.

Zhao, X. and Liu, X.: Global importance of secondary ice production, *Geophys. Res. Lett*., **48,** e2021GL092 581, 2021.